Journal of Materials Chemistry C

Accepted Manuscript

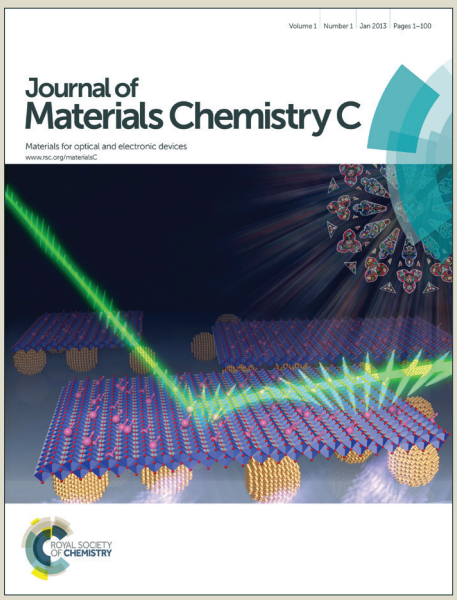

ROYAL SOCIETY OF CHEMISTRY

www.rsc.org/materialsC

Journal of Materials Chemistry C

Journal of Materials Chemistry C

Dynamic Article Links ►

ARTICLE TYPE

www.rsc.org/xxxxxx

Three-Colors Electrochromic Lithiated Vanadium Oxides: The Role of Surface Superoxide in the Electro-generation of Red State

S. Zanarini*[a], F. Di Lupo[a], A. Bedini[b], S. Vankova[a], N. Garino[a], C. Francia[a], S. Bodoardo*[a]

Received (in XXX, XXX) Xth XXXXXXXXX 20XX, Accepted Xth XXXXXXXXX 20XX

DOI: 10.1039/b000000x

Lithiated Vanadium oxides with polyelectrochromic behaviour are here reported for the first time. The electrochrome was obtained by means of a simple and solvent-free solid state reaction. Clear XPS evidences indicate that the electro-generation of red color is due to the dismutation of surface-adsorbed O_2^- species with subsequent formation of red colored V^{5+}-O_2^{2-} complexes. The reaction is switched electrochemically by oxidation of the surface V^{4+} centers.

The electrochromic behaviour of V^{5+} and V^{4+} oxides is well known.[1,2] The most commonly encountered Vanadium oxide is V_2O_5 that is yellow in its oxidised state (V^{5+}) and can intercalate Li^+ ions, when reduced to V^{4+} becoming blue. Vanadium oxides showing a red-orange colored phase, such as recently reported polyelectrochromic Mo and W doped Vanadium pentaoxide[3,4], are much less common.

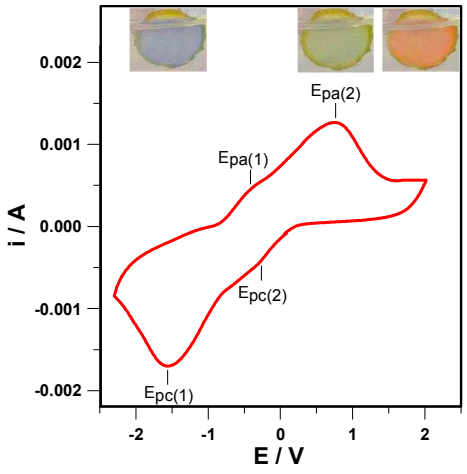

Figure 1. Typical CV of EFS deposited on FTO glass and colour appearance in the different potential regions. Scan rate: 0.1 V/s. Electrodes setup: EFS on FTO as working, Pt plate as counter and aqueous Ag/AgCl as reference. Electrolyte: 0.5 M Lithium Bis(Trifluoromethanesulfonyl)Imide(LiTFSi) in Propylene Carbonate(PC).

The practical uses of Vanadium oxides in electrochromic devices (ECD) have been however quite limited due to their low coloration efficiency, their partial water solubility (especially in acidic conditions)[5] and the need of sophisticated deposition techniques such as Sputtering to obtain optically performing thin films[6]. We report a water insoluble electrochromic material based on Lithiated Vanadium oxides, with Li^+ immobilized in the oxide structure, showing three different coloured states clearly detectable and electrochemically switchable, obtained by solid state synthesis. In a typical preparation, orthorhombic V_2O_5 reacted with Li hydroxide at 400 °C in nitrogen atmosphere. The as prepared powder (PS) was characterized by means of XRPD analysis (see Fig. S1), revealing the presence of several phases. In addition to un-reacted o-V_2O_5, two Lithiated compounds were identified: $Li_{0.3}V_2O_5$ (JCPDS No. 00-018-0755) and LiV_3O_8 (JCPDS No. 01-072-1193)[7]. The use of $Li_{0.3}V_2O_5$ as electrode material in lithium ion batteries is well known[8,9], moreover recently, due to its very low water solubility, it has been employed also in aqueous Li-ion batteries[10]. On the other hand its use as electrochromic material is reported here for the first time. To enrich the mixture on $Li_{0.3}V_2O_5$, a purification process, consisting in a simple precipitation in water, was necessary. PS powder was dispersed in ultrapure water and left to settle for 12 h then the supernatant was removed. The precipitate, reported hereafter as EFS (Electrochromic Fraction Sample), was dried in oven at 50 °C for 3 h. As evidenced by XRPD analysis, in comparison with PS (see fig S1), EFS resulted enriched on the $Li_{0.3}V_2O_5$ and LiV_3O_8 phases. More details on synthetic procedures and structural-morphological characterization are given in the S.I. FESEM images of PS and EFS are shown in Fig. S2. Observing the PS micrograph (see Fig. S2a) several morphologies are recognisable, indeed sub-micrometric grains are covered by nanowires structures. Conversely, EFS (Fig. S2b) shows only one defined morphology quite homogeneous in size and shape, constituted by micrometric particles with nanometric sub-structures. EFS powder exhibited the advantage to be easily dispersible in aqueous media. For this reason, to prepare the electrodes for further spectro-electrochemical testing, 3.5 mg of EFS sample were suspended in 0.4 mL of water and drop-casted on FTO glass. 20 µL of solution were employed to coat a masked circular area of 8 mm diameter. FESEM cross sections registered from 10 different equivalent samples (not shown) indicate that the thickness of EFS film on FTO was of 1.4±0.3 µm with a T%(500 nm) of circa 30 %. The typical Cyclic Voltammetry (CV) of EFS film on FTO together with its colour appearance in the different potential regions, is shown in Fig. 1. Similarly to

V_2O_5 thin films[1,2,11] two partially reversible redox processes are clearly visible at $\mathbf{E_{PC(1)}}$=-1.56 V, $\mathbf{E_{PA(1)}}$ =-0.46 V, $\mathbf{E_{PC(2)}}$ = -0.36 V and $\mathbf{E_{PA(2)}}$ = 0.76 V due to oxide phases interconversion[12].

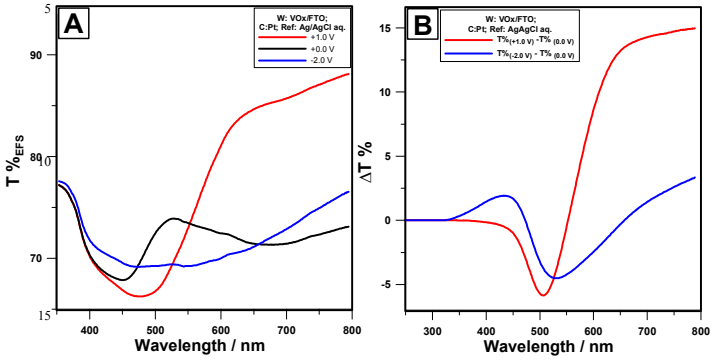

Figure 2. (A) UV-VIS absorption spectrum of FTO/EFS electrode after biasing at different potentials for 60s. FTO glass Baseline has been subtracted according to the following equation: $T\%_{EFS}= T\%_{FTO/EFS}+(100-T\%_{FTO})$. Cell setup and electrolyte is the same of Fig.1 (B) Modification of absorption spectrum in the 250-800 nm region by application of a positive (+1V) and negative (-2V) bias for 60 s with respect to 0 V. Potentials are vs. Ag/AgCl.

A net color change is easily observed by naked eye in correspondence of $\mathbf{E_{PA(2)}}$ (blue to yellow) and $\mathbf{E_{PC(1)}}$ peak (yellow to blue) while intermediate green color is electro-generated for $\mathbf{E_{PC(1)}} < \mathbf{E} < \mathbf{E_{PA(2)}}$ for the simultaneous presence of V^{5+} (yellow) and V^{4+} (blue) centers as confirmed by XPS analysis (see fig. S3). On the other hand the yellow to red-orange color transition is well visible for 1.5 V < **E** < 2. As described in more detail below, XPS analysis suggests that the formation of red-orange phase can be ascribed to an electrochemically-induced peroxide complexation (see Fig. 3 and scheme 1). As recently reported for Mo-doped and W-doped Vanadium pentaoxide[3,4] and unlike pure V_2O_5 our Lithiated material shows a red colored phase; comparing literature data on O_2^- XPS peak[13,14], the presence of superoxide is well visible in all samples except the pure V_2O_5 films[15]. Considering that superoxide cannot be further oxidized and that electrochemical oxidation can occur for V species in the reduced form as V^{4+} centers, the red color formation is a consequence of the well-known complexation of O_2^{2-} in V^{5+} centers[16] according to the following equation:

$$\underset{\text{YELLOW}}{V_2O_5} + 3\ O_2^{2-} \longrightarrow \underset{\text{RED-ORANGE}}{2\ VO_4^{3-}} + 3/2\ O_2(g)$$

Red phase generation is due to the dismutation of O_2^- species on the surface to O_2^{2-} and O_2 promoted by the electrochemical generation of V^{5+} close to thin layer-solvent interface (scheme 1).

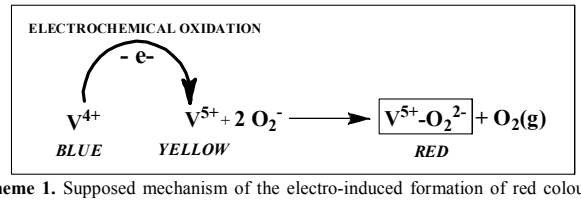

Scheme 1. Supposed mechanism of the electro-induced formation of red coloured state in Propylene Carbonate.

Similarly to a recent report[17] V^{5+} centers electro-generated close to surface-adsorbed O_2^- could act as dismutation catalyst and complexing agent for peroxide. The electro-generation of red-orange colored state, as the yellow one, is associated with the oxidation of V^{4+} to V^{5+} but with a certain kinetic delay; in fact surface V^{4+} species close to O_2^-, because of the limited ion diffusion in solid thin layer, require longer time to be oxidised than the ones proximal to FTO. In order to confirm this assessment, an experiment was performed by applying a fixed +1.5 V potential for 60 s: how presumed the same red-orange color was obtained by simply oxidizing V^{4+} to V^{5+} for a longer time. Despite the expected loss of gaseous oxygen in scheme 1 the formation of red color is reversible during repeated oxidative and reductive steps (see Fig. S6). This could be due to retention of O_2 on the EFS thin film and to the possible formation of O_2^- and O_2^{2-} species from O_2 and O_2^-during negative potential steps. As additional evidence cyclic voltammetric experiment depicted in Figure 1 was repeated by bubbling Ar with no effect on the shape of CV and on the formation of the three colors. An explanation could be again that the released gaseous O_2 is retained in the porous structure of the EFS. This experiment seemed also to suggests that the superoxide formation occurs most probably during the EFS preparation.

UV-VIS spectra of EFS film on FTO glass in the red-orange (+1 V vs. Ag/AgCl for 60 s), yellow-green (+0 V for 60 s) and blue colored states (-2 V for 60s) are shown in Fig. 2A. Figure 2B is a plot of **ΔT%** in the wavelength range of 250-800 nm during the transition from yellow to red (red line) and from yellow to blue (blue line). The 0 V spectrum is very similar to those reported in literature for thin layers of sputtered V_2O_5, supporting the assessment that our Lithiated material is essentially constituted by V^{5+} centers[12,18]. The transition from the yellow to blue state leads to a positive **ΔT%** in the 350 to 500 nm region, justifying the observed color change. The transition from the yellow to the red-orange state, analogously to the measurements reported for W and Mo-doped V_2O_5 [3,4] is associated with a noticeable increase of **ΔT%** in the 550-1500 nm range (see Fig. S4 for full range spectrum). This marked electro-induced increase of transparency in the red and NIR spectral region makes EFS thin films promising for application in infrared tunable optical filters as suggested by recent reports[19]. From Figure 2A it can be observed that in the 350-800 nm interval the maximum ΔT% was at 650 nm therefore wavelength was choosed to have the maximum sensitivity in time-related opto-electrochemical measurements. The estimate of EFS switching times on FTO glass (see fig. S5 for detailed electrodes and cell setup) was carried out by steps of positive and negative potentials, applied sequentially for several cycles according to the following program: E_1= +1 V, E_2= -2 V vs. Ag/AgCl; $t_1=t_2$=30 s. In Figure S6 the Transmittance Percent T%(650 nm) in PC/0.5 M LiTFSi is reported as function of time. By observing Figure S6 one can easily note that in general the bleaching process, occurring during electrochemical oxidation, is slower than the coloring process. In fact, according to the definition given in the S.I., we found Switching Time for 80 % Bleaching $\mathbf{ST_B}$ to be 11.2 s and for 80 % Coloring $\mathbf{ST_C}$ to be 3.7 s, having a maximum ΔT%(650nm) of 15.2. The contrast and switching times detected can be considered really good for a secondary electrochrome, in particular if it is taken into account

the very simple method used for its preparation: simple drop casting from a water suspension of the active material. The stability of bleached and colored states over repeated cycles is interesting: ΔT% between first and last cycle of ca. 2 % (See Fig. S6). The coloration efficiency for EFS on FTO glass, was estimated with the setup shown in figure S5, finding a η of -29 cm^2C^{-1}; this value is very similar to those reported in literature for V_2O_5 thin films produced by rf sputtering[1,2].

XPS spectra of EFS on glass FTO before potential application (black line) and after biasing for 60 s at +2 V (red line) or -2 V (blue line) are shown in Figure 3 (O1s lines) and Fig. S3 (V2p 3/2 lines). The multiplet splitting of the V2p 3/2 peak (Fig. S3a) indicates the presence of both V^{5+} (517.8 eV) and V^{4+} (516.6 eV) species[20,21] in the as prepared EFS. The application of positive or negative potentials affects the V^{5+}/V^{4+} ratio due to electrochemical interconversion of the two species. The area related to the V^{4+} species decreases from 38.17 to 14.38 eV after biasing with a potential of +2V (Fig. S3b) while increases to 49.50 after biasing a -2 V (Fig S3c). The O1s core level peak in as prepared EFS (Fig.3, A and B, black lines) splits into two peaks at 530.7 and 532.7 eV binding energies, ascribed to the the crystal lattice oxygen ions O^{2-} and to the chemisorbed superoxide O_2^- species, respectively[13,22]. The formation of the latter is caused by the stabilization of oxygen molecules on coordinatively unsaturated cation sites[15]. After biasing EFS at +2V, a reorganization of oxygen species occurs at crystal surface together with an increase of V^{5+}/V^{4+} ratio (Fig. 3 A). The area of the band at 532.7 eV (black curve) is significantly decreased and the area of the band at 530.27 eV (red curve) is significantly increased, due to the elimination of adsorbed O_2^- species and the formation of new vanadyl V^{5+}=O groups in the crystal lattice, respectively. After biasing EFS at -2V (Fig. 3B) a decrease of adsorbed O_2^- species is also observed (532.7 eV, black curve) together with an increase of lattice O^{2-} (530.06 eV, blue curve) but with the appearance of a new type of oxygen O^- species (531.6 eV, blue curve) adsorbed on the surface. According to XPS analysis of the as prepared EFS, it could be hence asserted that its surface is rich of O_2^- species (Fig. 3A,3B; black curve).

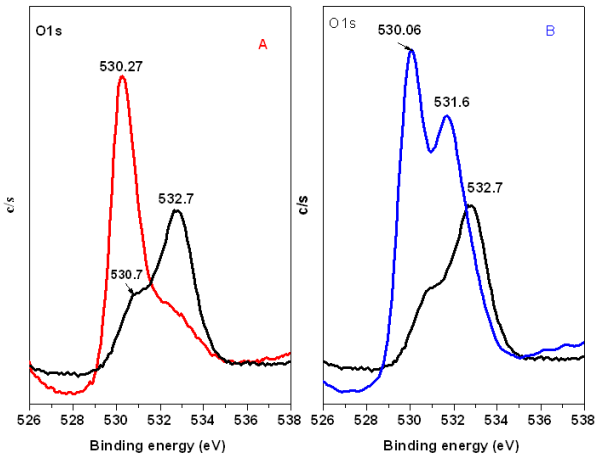

Figure 3. O1s X-ray photoelectron spectra of EFS on glass FTO collected from the sample before (black curves, part A and B) and after the application of +2V (red curve, part A) and -2V (blue curve, part B) for 60 s.

Actually, recent reports[15] have showed that superoxide species O_2^- are formed on the surface when metal species are not completely oxidized: this is the case of $Li_{0.3}V_2O_5$, the main EFS component, in which Vanadium oxidation state is +4.85 instead of 5 as for pure V_2O_5. When EFS is biased at negative potential (-2V) the following reactions occur as confirmed by the changes on the XPS spectra:

$$O_2^- + e^- \rightarrow 2O^-$$
$$O^- + e^- \rightarrow O^{2-}$$
$$V^{4+} + O^{2-} \leftrightarrow V^{4+}{=}O$$

The reduction of V^{5+} species to V^{4+} (Fig. S3c) is coupled with the reduction of superoxo O_2^- to O^- species[13] and with a subsequent reduction of O- to O^{2-} species[23]; finally a recombination occurs between V^{4+} and O^{2-} species leading to the formation of new V^{4+}-O groups at the surface of the oxide[24]. These reactions have been evidenced by the significant decrease of the intensity of the band of O_2^- species at 532.7 eV (Fig. 3B black curve) and by the appearance of a new band centered at 531.6 eV (Fig. 3B blue curve) related to the O^- species. The intensity of the band centered at about 530 eV (blue curve) increases with the reduction of O^- species to O^{2-} and the formation of V^{4+}=O groups.

Conclusions

The triple-color electrochromism of a mixture of Lithiated Vanadium oxides has been observed and explained here for the first time. The material was obtained by a simple and solvent-free solid state synthesis followed by precipitation in water. Polyelectrochromic thin films of tunable thickness can be easily produced via drop casting method on FTO glass. XPS analysis evidenced that the uncommon electro-generated red color phase is due to dismutation of surface superoxide, with complexation of peroxide in freshly generated V^{5+} centers. To produce the red colored state upon electrochemical oxidation a thin layer of V_2O_5 must contain on his surface a certain quantity of V^{4+} leading to superoxide formation in contact with atmosphere O_2. Lithiation or doping of Vanadium oxide structure with W or Mo are both effective methods to produce surface defects and thus to activate the red color state.

This research has been carried out in the context of the FP7 European Project ‘‘SMARTEC’’(ref. n. 258203). EU community is kindly acknowledged for the financial support.

[a] *GAME Lab, Dept. Applied Science and Technology - DISAT, Politecnico di Torino, Italy. Fax: +39 011 0904699; Tel: +39 011 0904641; E-mail: simone.zanarini@polito.it, silvia.bodoardo@polito.it*
[b] *Rockwood Italia S.p.A., Torino, Italy. Fax: +39 011 2269275; Tel: +39 011 2280501; E-mail: a.bedini@rpigments.com*

† Electronic Supplementary Information (ESI) available: Synthesis of PS and EFS samples and Deposition on FTO glass; Structural and Morfological Characterization; XPS analysis; Electrochemical and Spectro-Electrochemical Measurements; X-ray powder diffraction pattern of PS and EFS; FESEM micrographs; V2p3 XPS spectra; Full range UV-VIS absorption spectrum of EFS; Setup of customized optical glass cell for Spectro-Electrochemical measurements; Typical T%(650 nm) vs. time curve of FTO/EFS electrode during repeated potential switching cycles. See DOI: 10.1039/b000000x/

Notes and references

[1] C. G. Granqvist, *Handbook of Inorganic Electrochromic Materials*, 2002, Elsevier, Amsterdam.

[2] P. M. S. Monk, R. J. Mortimer, D. R. Rosseinsky, *Electrochromism And Electrochromic Devices*, 2007, Cambridge University Press, Cambridge.
[3] A. Jin, W. Chen, Q. Zhou, Z. Jian, *Electrochim. Acta*, 2010, **55**, 6408.
[4] Y. Yang, Q. Zhu, A. Jin, W. Chen, *Solid State Ionics*, 2008, **179**, 1250.
[5] S.F. Cogan, N.N. Nguyen, S.J. Perotti, R.D. Rauh, *J. Appl. Phys.*, 1989, **66**, 1333.
[6] S. Beke, *Thin Solid Films*, 2011, **519**, 1761.
[7] K.J. Rao, P.A. Ramakrishnan, R. Gadagkar *J Solid State Chem.*, 1999, **148**, 100.
[8] M.H. Bhat, B.P. Chakravarthy, P.A. Ramakrishnan, A. Levasseur, K.J. Rao, *Bull Mater Sci*., 2000, **23**, 461.
[9] D.O. Scanlon, A.Walsh, B.J. Morgan, G.W. Watson, *J. Phys. Chem. C*, 2007, **111**, 10707.
[10] J. Bao, M. Zhou, Y. Zeng, L. Bai, X. Zhang, K. Xu, Y. Xie, *J. Mater. Chem. A*, 2013, **1**, 5423.
[11] S. J. Perrotti, R. D. Rauh, *Proc. SPIE*, 1988, **1016**, 57.
[12] T.T.B. Nguyen, P.M. Tien, S. Badilescu, Y. Djaoued, L. Q. Nguyen *J. Appl. Phys.*, 1996, **80**, 7041.
[13] C. Balamurugan, D.-W. Lee, *Sens. Actuat. B*, 2014, **192**, 414.
[14]M.S.B. De Castro, C.L. Ferreira, R.R. de Avillez, *Infrared. Phys. Technol.*,2013, **60**, 103.
[15] M.A. Haija, S. Guimond, Y. Romanyshyn, A. Uhl, H. Kuhlenbeck, T.K. Todorova, M.V. Ganduglia-Pirovano, J. Döbler, J. Sauer, H.-J. Freund, *Surface Science*, 2006, **600**, 1497.
[16] R. Gopinath, B. Patel, *Org. Lett.*, 2000, **2**, 577.
[17] D. Zheng, Q. Wang, H.-S. Lee, X.-Q. Yang, D. Qu, *Chem. Eur. J.*, 2013, **19**, 8679.
[18] A. Talledo, A.M. Andersson, C. G Granqvist, *J. Appl. Phys.*, 1991, **69**, 3261.
[19] X-Y. Peng, B.Wang, J.Teng, J.B. Kana, X. Zhang, *Appl. Phys. Lett.*, 2013, **103**, 153503.
[20] M.Y. Shin, D.W. Park, J.S. Chung, *Appl. Catalysis B*, 2001, **30**, 409.
[21] E. Hryha, E. Rutqvist, L. Nyborg, *Surface Interface Analysis* 2012, **44**, 1022.
[22] Y. Kang, L. Wang, Y. Wang, H. Zhang, Y. Wang, D. Hong, S. Wang, *Sensors and Actuators B*, 2013, **177**, 570.
[23] R.H. Petrucci, W.S. Harwood, *General Chemistry, Principles and Modern Applications 9th edition*, 2006, Prentice Hall, p. 337.
[24] T.-D. Nguyen, T.-O. Do, *Langmuir*, 2009, **25**, 5322.